INSTITUTE OF PHYSICS PUBLISHING NONLINEARITY

Nonlinearity **16** (2003) 49–66 PII: S0951-7715(03)37558-9

A diffuse interface approach to Hele–Shaw flow

Karl Glasner[1]

Department of Mathematics, Duke University, Durham, NC 27708, USA

E-mail: glasner@math.duke.edu and kglasner@math.arizona.edu

Received 29 May 2002, in final form 1 October 2002
Published 28 October 2002
Online at stacks.iop.org/Non/16/49

Recommended by F Otto

Abstract

A diffuse interface model for the one-phase Hele–Shaw problem is derived from a gradient flow characterization due to Otto (1998 *Arch. Rat. Mech. Anal.* **141** 63). The resulting dynamical model yields a generalized form of Darcy's law, and reduces to a degenerate version of the well-known Cahn–Hilliard equation. Formal asymptotics illustrate the connection to the classical Hele–Shaw free boundary problem. Some example computations are carried out to demonstrate the flexibility of the modelling framework.

Mathematics Subject Classification: 76D27

1. Introduction

One of the most fundamental interface motions is that produced by a bubble of an incompressible, viscous fluid sandwiched between two narrowly spaced plates, a device known as the Hele–Shaw cell. Many variations of this experiment have been performed, producing a wide variety of morphologies. As a consequence, this experiment has served as a basis for the study of pattern formation in many contexts including dendritic solidification, porous media flow and diffusion-limited aggregation.

In this paper, we will concentrate on the one-phase problem, where a liquid bubble is surrounded by another fluid of negligible viscosity. In the classical sharp interface description, the fluid is immiscible and its velocity v obeys Darcy's law

$$v \propto \nabla p, \tag{1}$$

where p is the pressure. A timescale may be chosen so that the constant of proportionality in unity; we assume this throughout. Incompressibility requires that $\nabla \cdot v = 0$, or alternatively that the pressure satisfies the Laplace equation

$$\Delta p = 0. \tag{2}$$

[1] Present address: Department of Mathematics, University of Arizona, 617 North Santa Rita, PO Box 210089, Tucson, Arizona 85721, USA.

0951-7715/03/010049+18$30.00

On the interface Γ, the pressure must satisfy the Laplace–Young condition

$$p|_\Gamma = \gamma\kappa, \tag{3}$$

where γ is the surface energy, and κ is the curvature of the interface. The motion of the interface therefore derives from solving Laplace's equation on the domain occupied by the bubble subject to the boundary condition (3), and then determining the normal interface velocity

$$V_n = \nabla p|_\Gamma \cdot \hat{\boldsymbol{n}}, \tag{4}$$

where $\hat{\boldsymbol{n}}$ is the outward unit normal to the fluid interface. Obviously, this velocity law is highly non-local.

A considerable amount of mathematics has been generated about this problem. For the surface tension driven case various short-time existence results have been obtained [21,24,48]. In contrast, global existence in time is less-understood. Constantin and Pugh [18] have shown that solutions that are nearly circular will exist for all times, and will converge to circles. Considerable effort has gone into showing that this is not true in general, however; we discuss this in section 5.1.

A different characterization of Hele–Shaw flow has been given by Otto [37,44], by viewing the dynamics as a gradient flow of surface energy in an appropriate metric space. The notion of free boundary problems as gradient flows goes back to Fife [25] and has been discussed by Taylor and Cahn [50]. The metric space appropriate for the Hele–Shaw problem is endowed with the so-called 'Wasserstein' metric (sometimes called the L^2 Kantorovich distance), which can be interpreted in terms of the optimal transport problem of Monge [42].

One alternative to modelling a material interface as a infinitesimally narrow structure is to use a phase field approach, where the interface is spread out over a narrow transition region. Formal asymptotics may be used to demonstrate the equivalence of the two approaches, by considering the limit of a infinitesimally narrow diffuse interface. This idea has been successfully applied to a number of solidification problems (e.g. [13,53,54]). This notion has more recently been applied to fluid–fluid interfaces, such as in the work of Antanovskii [6], Chella and Vinals [16], Jacqmin [34,35], Gurtin *et al* [31], Lowengrub and Truskinovsky [41], and Anderson and McFadden [4].

The model derived here takes the form of a Cahn–Hilliard equation with concentration-dependent mobility $M(u)$,

$$u_t = \nabla \cdot (M(u)\nabla[f'(u) - \Delta u]), \tag{5}$$

where the potential $f(u)$ has (for example) minima at ± 1. The relationship between the constant mobility equation and its limiting interfacial dynamics was first shown by Pego [47]. For the case of constant mobility ($M \equiv 1$), the limiting interface motion is the so-called 'Mullins–Sekerka' problem. From a purely mathematical viewpoint, it can be considered as two-sided version of the problem studied here, but it is *not* the same as the model for Hele–Shaw flow with two fluids. There seems to be some confusion in the literature about this.

The connection between Cahn–Hilliard and Mullins–Sekerka dynamics was later demonstrated rigorously by Alikakos *et al* [1]. More recent studies (see [23] and the references therein) have considered the case where M is degenerate in each phase ($M(1) = M(-1) = 0$). In a certain limit, this model yields interfacial dynamics of motion by surface diffusion [14]. The distinguishing feature of our model is that only one-phase is degenerate, which makes the structure of equation (5) similar to equations describing thin fluid films (see, e.g. [9,43]).

Diffuse interface descriptions for Hele–Shaw flow with two fluids have appeared recently. A study by Folch *et al* [26] has proposed a phenomenological diffuse interface model based

upon the vortex sheet formulation of the Hele–Shaw problem, giving the correct sharp interface limit for the two-phase flow problem. Also, Lee *et al* [39, 40] have proposed a diffuse interface Hele–Shaw model based on the Navier–Stokes–Cahn–Hilliard system of Lowengrub and Truskinovsky [41]. Unlike the model discussed here, the fluid density in their model is entirely determined by the fluid composition.

This paper is laid out as follows. A review of the problem of optimal transport and its relationship to the Wasserstein metric is provided. Then a diffuse interface model is derived as a gradient flow of a free energy functional in this metric. This leads to an evolution equation which, under appropriate circumstances, has the one-phase Hele–Shaw problem as a singular limit. As an illustration of the model's usefulness and abilities, some computational examples are also provided. Finally, a rigorous connection between the evolution equation and gradient flows in the Wasserstein metric is given.

2. Optimal transport

In his 1781 paper, Monge [42] proposed a civil-engineering problem of moving mass from one configuration to another in an efficient manner. This problem was discussed further in a modern setting by Kantorovich [36]. It can be stated in terms of finding a map $M(x) : \Omega \to \Omega$, $\Omega \subset \mathbb{R}^n$, which moves particles at x to $M(x)$ in such a way as to reconfigure a density $\rho_0(x)$ into a density $\rho_1(x)$. Thus, the map $M(x)$ solves the 'Jacobian problem':

$$\rho_1(M(x)) \det \nabla M(x) = \rho_0(x). \tag{6}$$

It is natural to ask which of these maps is optimal, in that they minimize the functional

$$\int_\Omega |M(x) - x|^2 \rho_0(x)\, \mathrm{d}x. \tag{7}$$

It was shown by Brenier [11] among others (see also the review of Gangbo and McCann [27]) that the optimal map $M(x)$ is unique and the gradient of a convex function Ψ which (because of equation (6)) is the unique solution to the Monge–Ampere equation

$$\rho_1(\nabla \Psi(x)) \det \nabla^2 \Psi(x) = \rho_0(x). \tag{8}$$

Another characterization of this problem is given by the 'Wasserstein' distance (or metric) between ρ_0 and ρ_1. This can be stated as

$$d^2(\rho_1, \rho_2) = \inf_{p(x,y)} \int_\Omega \int_\Omega |x - y|^2 p(x, y)\, \mathrm{d}x\, \mathrm{d}y, \tag{9}$$

where the infimum is to be taken over the set

$$P = \left\{ p(x, y) \mid p \geqslant 0, \int_\Omega p(x, y)\, \mathrm{d}y = \rho_1(x), \int_\Omega p(x, y)\, \mathrm{d}x = \rho_2(y) \right\}. \tag{10}$$

The 'mass transfer function' $p(x, y)$ is, properly speaking, a Borel measure, which can be thought of as the unnormalized probability distribution of moving a particle at x to y. The minimizer obtained in (9) therefore corresponds, in a sense, to the most efficient way of moving material from one mass distribution to another. The connection between the integral in (9) and (7) can be made by setting $p(x, y) = \delta(y - M(x))$.

There is yet another, equivalent way of describing the Wasserstein metric by the 'hydrodynamic' interpretation given by Benamou and Brenier [8]. Given densities ρ_0, ρ_1, one may associate a velocity field $v(x, t)$ which move mass from configuration ρ_0 to ρ_1. In other words, $\rho(x, t)$, $v(x, t)$ satisfy the transport equation

$$\rho_t + \nabla \cdot (\rho v) = 0, \quad \rho(x, 0) = \rho_0(x), \quad \rho(x, 1) = \rho_1(x), \quad v \cdot n = 0 \qquad \text{on } \partial\Omega. \tag{11}$$

The cost functional may now be stated as the minimizer of an action integral.

Proposition 1 ([8]).

$$d^2(\rho_0, \rho_1) = \inf_{\rho, v} \int_0^1 \int_\Omega \rho |v|^2 \, \mathrm{d}x \, \mathrm{d}t, \tag{12}$$

where $\rho(x, t)$, $v(x, t)$ satisfy (11).

The optimum path $\rho(x, t)$ through density space is, roughly speaking, the geodesic between ρ_0 and ρ_1.

It is possible to explicitly state the metric tensor for (9) with some stipulations attached. In section 6, the following result is established.

Theorem 1. *Suppose that Ω is a bounded region with a smooth boundary, and suppose that $\rho_0, \psi \in C^{1,\alpha}(\Omega)$ and $\rho_0 > 0$. Then*

$$\lim_{\epsilon \to 0} \frac{d^2(\rho_0, \rho_0 + \epsilon\psi)}{\epsilon^2} = \int_\Omega \rho_0 |\nabla \Phi|^2 \, \mathrm{d}x, \tag{13}$$

where Φ is a solution to the elliptic equation

$$-\nabla \cdot (\rho_0 \nabla \Phi) = \psi, \qquad \frac{\partial \Phi}{\partial n} = 0 \tag{14}$$

which is unique up to a constant.

The right-hand side of (13) describes a bilinear, symmetric form on ψ which we shall label $g_\rho(\psi, \psi)$, and can be equivalently written as the inner product

$$g_\rho(\psi, \psi) = \int_\Omega \psi \mathcal{L}_\rho^{-1} \psi \, \mathrm{d}x, \tag{15}$$

where the positive, self-adjoint operator is defined by

$$\mathcal{L}_\rho \psi = -\nabla \cdot (\rho \nabla \psi), \tag{16}$$

and its inverse is accompanied by a Neumann boundary condition.

Let us briefly describe a formal argument which leads to this. It is reasonable to suppose that all possible minimizing pairs (ρ, v) of (12) satisfy

$$\rho(x, t) = \rho_0(x) + \mathcal{O}(\epsilon), \tag{17}$$

$$v(x, t) = \epsilon V(x, t) + \mathcal{O}(\epsilon^2). \tag{18}$$

By integrating (11) from 0 to 1 in time, we see that at leading order, $V(x, t)$ will satisfy the constraint

$$\psi + \nabla \cdot \left(\rho_0(x) \int_0^1 V(x, t) \, \mathrm{d}t \right) = 0. \tag{19}$$

For small ϵ, the problem is to minimize the functional

$$\int_0^1 \int_\Omega \rho_0(x) |V|^2 \, \mathrm{d}x \, \mathrm{d}t \tag{20}$$

for vector fields $V(x, t)$ which satisfy the constraint (19).

Consider the space of smooth velocity fields with vanishing normal component on the boundary

$$Q = \{v(x, t) | v : \Omega \times [0, 1] \to \mathbb{R}^n, \, v \cdot n = 0 \text{ on } \partial\Omega\}. \tag{21}$$

A weighted Helmholtz-type orthogonal decomposition is $Q = D \oplus G$, where

$$D = \left\{ v \in Q \mid \nabla \cdot \left(\rho_0 \int_0^1 v(x,t)\,\mathrm{d}t \right) = 0 \right\}, \tag{22}$$

$$G = \{ v \in Q \mid v = \nabla \Phi(x) \}. \tag{23}$$

Indeed, for a given $v \in Q$, let Φ solve the elliptic problem

$$-\nabla \cdot (\rho_0 \nabla \Phi) = \nabla \cdot \left(\rho_0 \int_0^1 v\,\mathrm{d}t \right), \qquad \frac{\partial \Phi}{\partial n} = 0. \tag{24}$$

Then we may write $v = \nabla\Phi + w$, and it is easy to see that $w \in D$. Orthogonality of the decomposition is with respect to the weighted inner product

$$\langle u, v \rangle = \int_0^1 \int_\Omega \rho_0 u \cdot v\,\mathrm{d}x\,\mathrm{d}t \tag{25}$$

and follows by an application of Green's theorem.

Now consider the minimization problem (20) together with the constraint (19). Suppose that V is the minimizer and let $V(x,t) + \delta V(x,t)$ be a perturbation which also satisfies the constraint (19). Since the constraint is linear, it follows that

$$\nabla \cdot \left(\rho_0 \int_0^1 \delta V\,\mathrm{d}t \right) = 0. \tag{26}$$

In other words, $\delta V \in D$. The first variation of the functional in (20) is stationary for all admissible perturbations, which means that

$$\inf_V \int_0^1 \int_\Omega \rho_0(x) V \delta V\,\mathrm{d}x\,\mathrm{d}t = 0, \qquad \delta V \in D. \tag{27}$$

As a consequence of the orthogonality of D and G, it follows there is some $\Phi(x)$ so that $V(x,t) = \nabla\Phi(x)$, and using (19) we find that Φ solves (up to a constant) equation (14). Inserting the minimizer back into the functional in (20) yields (13).

3. Abstract gradient flows and a diffuse interface model

A gradient flow on a manifold may be written in terms of a metric tensor $g_\rho(\psi_1, \psi_2)$ as the differential equation

$$g_\rho(\rho_t, \psi) = -\langle \delta F, \psi \rangle, \qquad \text{for all } \psi \in T_\rho, \tag{28}$$

where T_ρ is the tangent space at the point ρ, and $\langle , \rangle$ is the action of the linear functional given by the first variation of F on a member of the tangent space. In our context, ρ will be the density configuration which the inner product $g_\rho(\cdot,\cdot)$ depends on.

Otto [44–46] has made extensive use of the Wasserstein metric as a basis for describing many familiar evolution equations as abstract gradient flows. In particular, he characterized the sharp interface Hele–Shaw evolution [44] as a gradient flow of surface energy in a space which is endowed with the Wasserstein metric.

Our goal here is to make use of this notion in the context of a diffuse interface description. The manifold for our evolution equations will be composed of positive density functions $\rho(x) \in H^1(\Omega)$ which have constant prescribed total mass

$$\int_\Omega \rho(x)\,\mathrm{d}x = \text{const}. \tag{29}$$

Using the explicit form of the metric tensor given in (15), the gradient flow of a particular energy functional $F(\rho)$ is then given by

$$\int_\Omega \psi \mathcal{L}_\rho^{-1} \rho_t = -\int_\Omega \delta F \, \psi \, \mathrm{d}x \tag{30}$$

for all ψ in the tangent space, which is identified as

$$T_\rho = \left\{ \psi \in H^1(\Omega) \Big| \int_\Omega \psi(x) \, \mathrm{d}x = 0 \right\}. \tag{31}$$

Therefore, the quantity $\mathcal{L}_\rho^{-1}\rho_t + \delta F$ is in the orthogonal complement (with respect to the L^2 inner product) of the tangent space, which is just the set of constant functions, i.e.

$$\mathcal{L}_\rho^{-1}\rho_t + \delta F = \text{const}. \tag{32}$$

Assuming that δF is smooth enough, applying $\mathcal{L}_\rho$ to this equation gives the evolution equation

$$\rho_t = \nabla \cdot (\rho \nabla \delta F). \tag{33}$$

We will now propose a model for the free energy as a functional of the density of the liquid:

$$F(\rho) = \int \frac{k}{2} |\nabla \rho|^2 + \rho \tilde{f}(\rho) \, \mathrm{d}x, \tag{34}$$

where $\tilde{f}(\rho)$ is the free energy density per unit mass and the integral is taken over a physical domain Ω. The non-classical gradient energy term was first utilized long ago by van der Waals [52] and Korteweg [38], and has appeared in modern context in various diffuse interface models (see, e.g. [15]). To simplify notation, we will use

$$f(\rho) = \rho \tilde{f}(\rho). \tag{35}$$

It is supposed that f has exactly two minima (see figure 1) at ρ_a and ρ_b. The evolution equation (33) then is the fourth-order degenerate parabolic equation

$$\rho_t = \nabla \cdot (\rho \nabla [f'(\rho) - k\Delta\rho]). \tag{36}$$

This is the Cahn–Hilliard equation [15] with a mobility equal to ρ.

The conditions on the physical boundary will be

$$\nabla \rho \cdot \hat{\boldsymbol{n}} = 0, \tag{37}$$

$$\rho \nabla [f'(\rho) - k\Delta\rho] \cdot \hat{\boldsymbol{n}} = 0. \tag{38}$$

The first is a consequence of energy minimization, where we have assumed that there is no surface energy associated with the domain walls (Jacqmin [35] has treated contact lines in a diffuse interface setting by including energy terms for the physical boundaries as well). The second boundary condition enforces no flux at the boundary. In the case that the domain is unbounded, a condition specifying the flux at infinity could be imposed instead.

Notice that equation (36) may be written in conservation form as

$$\rho_t + \nabla \cdot j = 0, \tag{39}$$

$$j = -\nabla \cdot \boldsymbol{T}, \tag{40}$$

where the stress $\boldsymbol{T}$ is

$$\boldsymbol{T} = -k\left[\left(\rho\Delta\rho + \tfrac{1}{2}|\nabla\rho|^2\right)\boldsymbol{I} - \nabla\rho \otimes \nabla\rho\right] + (\rho f' - f)\boldsymbol{I}. \tag{41}$$

The first term is the negative Korteweg stress tensor $\boldsymbol{K}$, which describes capillary forces associated with the variations of density. This term has appeared in other diffuse interface

descriptions of fluids (see the review [5]) as an extra stress incorporated into the balance law for momentum. The last term in (41) is nothing more than the thermodynamic pressure, using the standard relation

$$p = \rho^2 \tilde{f}'(\rho) = \rho f'(\rho) - f(\rho). \tag{42}$$

As a consequence, we may view equation (40) as the 'generalized Darcy's law' for a fluid with a diffuse interface.

The fact that equation (36) is a degenerate diffusion equation poses some mathematical difficulty if ρ becomes zero. Existence of weak, non-negative solutions has been established by Elliott and Garcke [23] for a Cahn–Hilliard equation with a similar degeneracy. Uniqueness for these sort of equations is, on the other hand, presently not known. As will be shown in the next section, the degeneracy is crucial to obtain the 'one-sided' free boundary problem limit. On the other hand, we will assume that solutions remain positive, and no mathematical singularities are encountered.

4. Sharp interface limit

When the gradient energy is small, we may expect that the our model will develop narrow transition layers connecting regions of differing density. We will show how the limiting behaviour is connected to the sharp interface Hele–Shaw problem.

Through equilibrium considerations, the surface energy and width of the diffuse interface may be derived. Consider a one-dimensional, steady solution of (36), which using the no-flux boundary condition must solve

$$f'(\rho) - k\rho_{xx} = \mu^*, \tag{43}$$

where μ^* is a constant of integration. It is assumed that at infinity, the density approaches constants yet to be determined:

$$\rho \to \rho_a, \qquad x \to -\infty, \tag{44}$$

$$\rho \to \rho_b, \qquad x \to \infty. \tag{45}$$

A further integration of (43) gives

$$\frac{k}{2}\rho_x^2 = f(\rho) - f(\rho_a) - \mu^*(\rho - \rho_a) \equiv f_\mu(\rho), \tag{46}$$

where the condition at $-\infty$ has been used. The quantities ρ_a, ρ_b and μ must be chosen so that $f'_\mu(\rho_{a,b}) = 0$ in order to satisfy conditions (44) and (45). This can be done in a unique way, using the standard 'common tangent' (or Maxwell) construction (figure 1). Then equation (46) may be integrated again to yield an increasing solution $\rho_0(x)$ which describes the equilibrium density profile.

As in other phase field theories [12], there is an equipartition of energy between the first and second terms in (34), so that the energy associated with an equilibrium transition layer, i.e. the surface energy, is the integral

$$\gamma = k\int_{-\infty}^{\infty} (\rho_0)_x^2 \,\mathrm{d}x = 2\int_{-\infty}^{\infty} f_\mu(\rho_0)\,\mathrm{d}x. \tag{47}$$

The width of the interface may be defined to be

$$\epsilon = \frac{k(\rho^*)^2}{\gamma}, \tag{48}$$

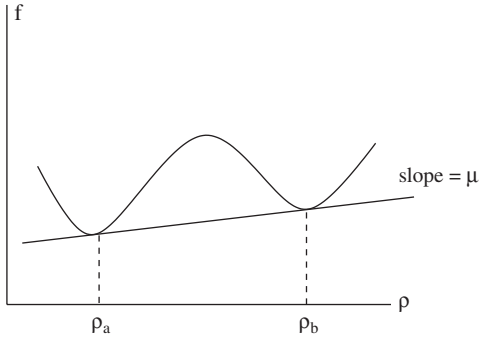

Figure 1. The common tangent construction. The line is tangent to the graph of the free energy at two points ρ_a, ρ_b. The slope of this line is μ, which ensures that f'_μ is zero at both ρ_a and ρ_b.

where ρ^* is a characteristic mass density so that ϵ has a dimension of length. This definition is, of course, somewhat arbitrary, and since we are only concerned about the limit as $\epsilon \to 0$, ρ^* may be set to unity. Notice that the rescaled equilibrium solution $\psi(z) = \rho_0(\epsilon z)$ will satisfy

$$\int_{-\infty}^{\infty} \psi_z^2(z)\,\mathrm{d}z = \frac{k}{\gamma}\int_{-\infty}^{\infty} (\rho_0)_x^2\,\mathrm{d}x = 1. \tag{49}$$

The free energy may now be rewritten

$$F(\rho) = \gamma \int \frac{\epsilon}{2}|\nabla\rho|^2 + \frac{1}{\epsilon}g(\rho)\,\mathrm{d}x, \tag{50}$$

where

$$g(\rho) = \frac{\epsilon}{\gamma}f(\rho). \tag{51}$$

For the analysis, it will be convenient to rewrite the equation as the coupled system

$$\frac{\mu}{\gamma} = g'(\rho) - \epsilon^2\Delta\rho, \tag{52}$$

$$\epsilon\rho_t = \nabla\cdot(\rho\nabla\mu). \tag{53}$$

A solution for small ϵ will now be sought. The analysis proceeds like that of Pego [47] for the constant mobility Cahn–Hilliard equation. In order to avoid the singularity associated with $\rho \to 0$, we will take the vapour density to be small but positive:

$$0 < \rho_a = \mathcal{O}(\epsilon). \tag{54}$$

To incorporate this into the description of the rescaled bulk free energy $g(\rho)$, we will suppose that we can expand g as

$$g(\rho) = g_0(\rho) + \epsilon g_1(\rho) + \cdots, \tag{55}$$

where the double-well function g has minima at ρ_b and 0, and g_1 satisfies

$$g_1(\rho_b) = g_1(0), \qquad g_1'(0) < 0. \tag{56}$$

A function g can be constructed which satisfies these conditions; see equation (72).

We suppose there are two subregions, $\Omega_b(t)$ and $\Omega_a(t)$, separated by the level set $\Gamma = \{x \mid \rho(x) = \frac{1}{2}(\rho_a + \rho_b)\}$, where Ω_b corresponds to the denser fluid region where $z > 0$. Near the interface, we use a local orthogonal coordinate system (z, s), where s denotes

the distance along Γ and z is the signed distance to Γ rescaled by a factor of ϵ^{-1}. The equations in the new coordinates are

$$\epsilon^2\rho_z r_t + \epsilon^3(\rho_t + \rho_s s_t) = (\rho\mu_z)_z + \epsilon\rho\Delta r\mu_z + \epsilon^2[\rho\Delta s\mu_s + |\nabla s|^2(\rho\mu_s)_s], \tag{57}$$

$$\frac{\mu}{\gamma} = g'(\rho) - [\rho_{zz} - \epsilon\Delta r\rho_z - \epsilon^2(\Delta s\rho_s + |\nabla s|^2\rho_{ss})]. \tag{58}$$

The dependent variables are expanded in regular power series in ϵ, i.e. $\rho = \rho^{(0)} + \epsilon\rho^{(1)} + \epsilon^2\rho^{(2)} + \cdots$, both near and away from the interface. The solutions must agree on an intermediate scale, leading to the 'matching' conditions (see [13])

$$\rho^{(0)}(z) \sim \rho^{(0)}(\pm 0), \qquad z \to \pm\infty, \tag{59}$$

$$\rho^{(1)}(z) \sim \rho^{(1)}(\pm 0) + \rho_r^{(0)}(\pm 0)z, \qquad z \to \pm\infty, \tag{60}$$

$$\rho^{(2)}(z) \sim \rho^{(2)}(\pm 0) + \rho_r^{(1)}(\pm 0)z + \rho_{rr}^{(0)}(\pm 0)z^2, \qquad z \to \pm\infty, \tag{61}$$

with similar conditions for μ. The variables on the left are a part of the inner expansion, and those on the right-hand side are part of the outer expansion. The notation $f(\pm 0)$ means the limit of this quantity from one side of the interface.

At leading order, the inner solution solves

$$\left(\rho^{(0)}\mu_z^{(0)}\right)_z = 0, \qquad g_0'(\rho) - \rho_{zz}^{(0)} = \frac{\mu^{(0)}}{\gamma}. \tag{62}$$

Using the matching condition (59), we see that $\mu^{(0)}$ only depends on s and t. The other equation's solution must therefore be the equilibrium solution denoted by $\rho^{(0)} = \psi(z)$ as discussed above. In particular, the common-tangent construction implies (note that $\rho_a = 0$ by the choice of g_0)

$$g'(0) = g'(\rho_b) = \frac{g(\rho_b) - g(0)}{\rho_b} = \frac{\mu^{(0)}}{\gamma}. \tag{63}$$

The outer solutions in the dense phase Ω_b will solve

$$g'(\rho^{(0)}) = \mu^{(0)}, \qquad \nabla\cdot(\rho^{(0)}\nabla\mu^{(0)}) = 0 \tag{64}$$

subject to the boundary conditions (37), (38) as well as the matching condition (59). The unique solutions are therefore simply constants, with $\rho^{(0)} = \rho_b$.

To order ϵ, the inner region equations are

$$(\psi\mu_z^{(1)})_z = 0, \qquad \mathcal{L}\rho^{(1)} = \frac{\mu^{(1)}}{\gamma} - \kappa^{(0)}\psi + g_1'(\psi), \tag{65}$$

where $\mathcal{L} = g''(\psi) - \mathrm{d}^2/\mathrm{d}z^2$. The leading order curvature of the interface $\kappa^{(0)}$ has been identified with $-\Delta r$, with the convention that if Ω_b is convex, the curvature is positive. Using (65*b*) and the matching condition for $\mu^{(1)}$, we find that $\mu^{(1)}$ is independent of z. The other equation has a solvability condition

$$\rho_b\mu^{(1)} = \gamma\kappa^{(0)}\int \psi_z^2\,\mathrm{d}z + \gamma\int_{-\infty}^{\infty} g_1'(\psi)\psi_z\,\mathrm{d}z. \tag{66}$$

The second integral is zero by virtue of (56*a*), and because of (49), the solvability condition may be written

$$\rho_b\mu^{(1)} = \gamma\kappa^{(0)}. \tag{67}$$

The outer solution $\mu^{(1)}$ in the dense phase Ω_b will solve

$$\Delta\mu^{(1)} = 0, \tag{68}$$

which is subject to the Neumann boundary conditions on the physical boundary and the Dirichlet condition at the interface provided by (67).

The inner expansion to $\mathcal{O}(\epsilon^2)$ gives

$$V^{(0)}\rho_z^{(0)} = \left(\rho^{(0)}\mu_z^{(2)}\right)_z, \tag{69}$$

where the leading order velocity $V^{(0)}$ has been identified with r_t. The matching condition (61) for μ yields in this case

$$\mu_r^{(1)}(\pm 0) = \mu_z^{(2)}(\pm z), \qquad z \to \pm\infty. \tag{70}$$

Integrating equation (69) from $-\infty$ to ∞ gives

$$V_0\rho_b = \rho_b\mu_r^{(1)}(+0). \tag{71}$$

Equating the quantity $\rho_b\mu^{(1)}$ with the pressure p, equations (67), (68a) and (71) constitute the free boundary problem described in the introduction.

5. Numerical examples

In this section, we demonstrate some computations using the diffuse interface model to illustrate its usefulness to study problems with Hele–Shaw dynamics. The principle advantage over methods which track the moving free boundary (e.g. [32, 51]) is that the fluid interface is represented by a level set of the field ρ (as in the sharp interface limit) whose motion is implicit in the PDE dynamics.

In the examples below, we choose a simple, polynomial form for $g(\rho)$, namely

$$g(\rho) = (\rho - \rho_a)^2(\rho - \rho_b)^2. \tag{72}$$

We set $\rho_b = 1$, and consistent with (56) and the formal sharp interface limit obtained, ρ_a is set to be ϵ. Having a non-zero ρ_a is similar to the effect of the 'precursor film' regularization which is used for degenerate fourth-order equations describing motion of thin films [19]. The surface tension, which only determines the timescale for evolution, is set to unity.

Finite-element algorithms for degenerate fourth-order equations have been proposed by Barrett, Blowey and Garcke [7] and Grün [30] among others. We adopt a simpler operator splitting approach, which utilizes a finite difference approximation in space and is semi-implicit in time. The first-order time stepping method reads

$$\epsilon\frac{\rho_{n+1} - \rho_n}{\Delta t} + \epsilon^2 M\Delta^2\rho_{n+1} = \epsilon^2\nabla\cdot((M - \rho_n)\nabla\Delta\rho_n) + \nabla\cdot(\rho_n\nabla g'(\rho_n)), \qquad M = \sup\rho_n. \tag{73}$$

Unconditional stability of this method has recently been demonstrated [10]. Semi-implicit schemes like this one for second-order parabolic equations go back to Douglas and Dupont [20]. A similar approach for fourth-order order parabolic equations describing surface diffusion has recently been proposed by Smereka [49].

The spatial operators in (73) were computed using standard, second-order accurate stencils. This allows for a discrete Fourier transform to be used to invert the constant-coefficient linear operator which acts on ρ_{n+1} in (73). The resulting algorithm is consequentially very fast, even when small time steps are used.

As in all diffuse interface methods, there is a constraint on the spatial resolution Δx of the form

$$\Delta x \leqslant C\epsilon. \tag{74}$$

This requirement really states that enough grid points must be used to properly resolve the transition layer. In the simulations here, Δx was chosen so that there were about five grid points

across the layer. It turns out that in many problems, it is possible to make a transformation of the equations [28] which considerably enlarges the constant C in (74).

5.1. Example: break up of a bubble

We consider the evolution of a long, narrow bubble. Surface tension acts to reduce the perimeter, but the final state is not just a single circle, but several of them (see figure 2), which results from pinch-off of thin necks which develop in the fluid.

The possibility of topological changes as seen here has been the subject of considerable attention [2, 3, 17, 22, 29]. It is accepted that such events should happen in the sharp interface model, but no rigorous proof of this exists. The sharp interface model encounters a singularity at the point of break up, and continuation past this point is not easily accomplished with a front tracking method. The diffuse interface model, however, is completely insensitive to such events, and provides a unique way of continuing the solution past the breakup point.

5.2. Example: a ferrofluid

An interesting variation of the Hele–Shaw experiment has been performed with a *ferrofluid*, a colloidal suspension of paramagnetic particles, which is subject to a uniform magnetic field

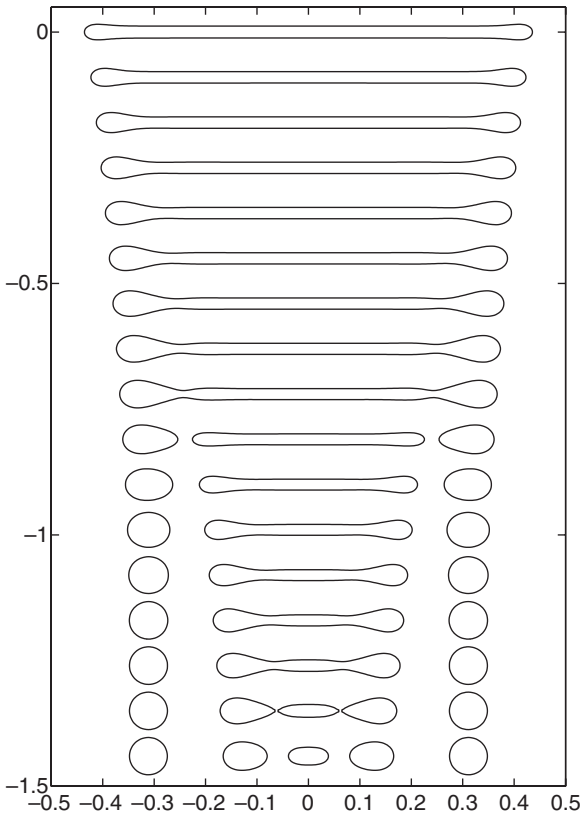

Figure 2. Evolution of a long, narrow bubble. Several break-up events occur, leading eventually to an array of circular bubbles. In this computation, $\epsilon = 0.005$ and the grid was 256×64 with a resolution of $\Delta x = 1/256$. Plotted are the level curves $\rho = 1/2$.

perpendicular to the plates. More detail about this problem may be found in [33, 44] and the references therein.

Our model can easily be extended to describe this experiment by adding to the free energy (34) a term describing magnetic energy

$$F_{\mathrm{M}}(\rho) = 2\pi M^2 \int \rho k_b * \rho \, \mathrm{d}x, \tag{75}$$

where M is the magnetization and the convolution kernel k_b is

$$k_b = \frac{1}{b^2} k\left(\frac{x}{b}\right), \qquad k(x) = \frac{1}{2\pi}\left(\frac{1}{|x|} - \frac{1}{(|x|^2+1)^{1/2}}\right), \tag{76}$$

where b is the plate spacing. By a calculation similar to that in section 3, this extra energy gives an additional term in the evolution equations:

$$\epsilon \rho_t = \nabla \cdot (\rho \nabla [g'(\rho) - \epsilon^2 \gamma \Delta \rho + \epsilon (4\pi M^2) k_b * \rho]). \tag{77}$$

A non-dimensional quantity associated with this problem is the magnetic Bond number

$$N_B = \frac{2M^2 b}{\gamma}. \tag{78}$$

As N_B is increased, the circular bubble equilibrium solution for this problem becomes unstable. The ensuing dynamics can be quite complicated, and eventually a convoluted steady state structure emerges. In real experiments, it is even possible that a single bubble disintegrates into many smaller shapes.

The numerical algorithm is similar to (73). The convolution term was computed using its discrete-Fourier representation at time n and was simply added to the right-hand side of (73).

Figure 3 shows the initial evolution of a slightly deformed circle. The final, steady state shape is shown in figure 4.

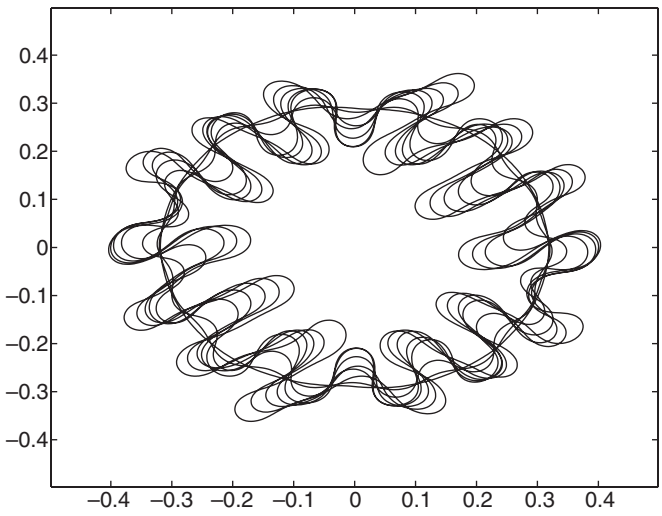

Figure 3. Instability of a near-circular bubble of a magnetic fluid. The Bond number is 3.5 and $b = 0.1$. In this computation, $\epsilon = 0.005$, the grid was 256×256 with $\Delta x = 1/256$.

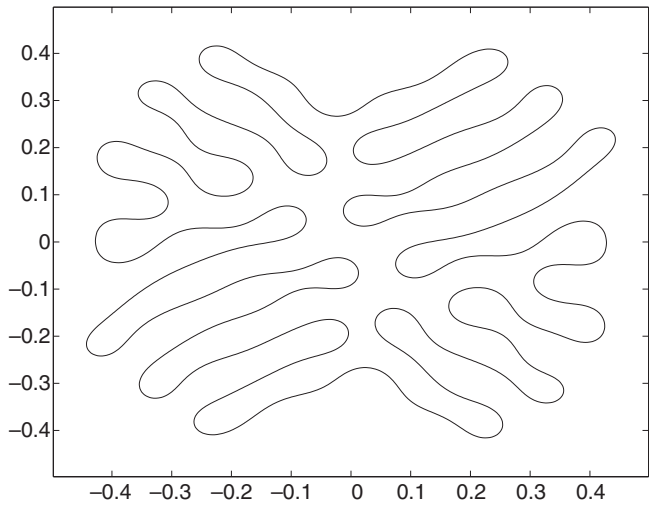

Figure 4. 'Labyrinthine' pattern generated as the steady state of the evolution in figure 3.

Appendix. Proof of theorem 1

In the proof of proposition 1, Benamou and Brenier showed that the velocity field which is optimal for (12) is one that is constant along Lagrangian paths. In other words, if $M(x)$ is the optimal map, then the optimal velocity field is one which sends particles directly from x to $M(x)$ along a straight line. In terms of the Lagrangian coordinate y, this means that

$$v(y) = M(y) - y. \tag{79}$$

In particular, the cost associated with this minimizer is (in Lagrangian coordinates)

$$d^2(\rho_0, \rho_1) = \int_\Omega \rho_0(y)|v(y)|^2 \,\mathrm{d}y. \tag{80}$$

Conversely, if $\bar{v}(y)$ is the gradient of a scalar and $\rho(x, t)$ evolves by following Lagrangian paths given by $\bar{v}(y)$, then $\bar{v}(y)$ is in fact optimal for (12). More precisely,

Proposition 2. *Suppose $\bar{v}(y) = \nabla\Pi(y)$ and is sufficiently smooth, and let the Lagrangian trajectories be*

$$x(y, t) = y + t\bar{v}(y), \tag{81}$$

which (for small $\bar{v}$) has an inverse $y(x, t) = x$. Let $\rho(x, t)$ solve ($11_{a,b}$) with

$$v(x, t) = \bar{v}(y(x, t)). \tag{82}$$

Then

$$d^2(\rho(x, 0), \rho(x, 1)) = \int_\Omega \rho_0(y)|\bar{v}(y)|^2 \,\mathrm{d}y. \tag{83}$$

Proof. If $\bar{v}(y)$ is indeed the optimal velocity field for (12), then (83) is the same as (80). We will show that $\bar{v}(y)$ is optimal by showing that

$$\Psi(y) = \Pi(y) + \tfrac{1}{2}|y|^2 \tag{84}$$

is the unique solution of the Monge–Ampere equation (8) and therefore (79) implies that $\bar{v}(y) = \nabla\Pi(y) = \nabla\Psi(y) - y$ must be optimal.

Equation (11) is, in Lagrangian coordinates

$$\frac{\partial}{\partial t}\rho(y,t)+\rho(y,t)(\nabla_x\cdot v)(y,t)=0, \tag{85}$$

where $\nabla_x\cdot v$ is the divergence with respect to the Eulerian coordinate. This may be integrated to give

$$\rho(y,t)=\rho_0(y)\exp\left(\int_0^t(\nabla_x\cdot v)(y,t)\,\mathrm{d}t\right). \tag{86}$$

Then

$$\nabla_x\cdot\bar{v}(y(x,t),t)=\nabla v(y):\nabla y(x,t)=\nabla\Pi(y)^2:\nabla y(x,t) \tag{87}$$

and by differentiating (81) with respect to x, we obtain

$$\nabla_x y(x,t)=[I+t\nabla^2\Pi(y)]^{-1} \tag{88}$$

and therefore

$$\nabla_x\cdot\bar{v}(y(x,t),t)=\nabla^2\Pi(y):[I+t\nabla^2\Pi(y)]^{-1}=\mathrm{tr}(\nabla^2\Pi(y)[I+t\nabla^2\Pi(y)]^{-1}). \tag{89}$$

We now demonstrate the following identity for a matrix A:

$$\exp\left(\int_0^t\mathrm{tr}(A(I+tA)^{-1})\right)=\det(I+tA). \tag{90}$$

Letting λ_i, $i=1,\ldots,n$ be the eigenvalues of A, we have

$$\begin{aligned}\exp\left(\int_0^t\mathrm{tr}(A(I+tA)^{-1})\right)&=\exp\left(\int_0^t\sum_{i=1}^n\frac{\lambda_i}{1+t\lambda_i}\,\mathrm{d}t\right)\\&=\exp\left(\sum_{i=1}^n\ln(1+t\lambda_i)\right)\\&=\prod_{i=1}^n(1+t\lambda_i)=\det(I+tA).\end{aligned} \tag{91}$$

Now set $t=1$, and use the matrix identity (90) in conjunction with (86) and (89) to give

$$\rho(y,1)=\rho_0(y)\det(I+\nabla^2\Pi(y)). \tag{92}$$

Using (81) and (84) this is the same as

$$\rho(\nabla\Psi(y),1)=\rho_0(y)\det(\nabla^2\Psi(y)) \tag{93}$$

which is equation (8) as desired.

The proof of the theorem contains two parts: an upper and lower bound. In what follows, generic constants independent of ϵ will be denoted by C.

Upper bound. Consider $\rho(x,t)$ given by

$$\rho(x,t)=\rho_0+\epsilon t\psi(x). \tag{94}$$

Associate with this density evolution, the velocity field given by $v(x,t)=\nabla\Pi(x,t)$ where Π is the solution (up to a constant) of

$$-\nabla\cdot(\rho\nabla\Pi)=\epsilon\psi,\qquad\frac{\partial\Pi}{\partial n}=0. \tag{95}$$

Notice that ρ and v satisfy condition (11). According to the usual elliptic estimates, the following hold:

$$\|\Pi\|_{C^{2,\alpha}} \leqslant \epsilon C\|\psi\|_{C^{0,\alpha}}, \qquad \|v\|_{C^{1,\alpha}} \leqslant \epsilon C\|\psi\|_{C^{0,\alpha}} \tag{96}$$

independent of t. Let $\Pi = \epsilon\Phi + \Pi'$, where Φ is given by (14). Using (14) and (95) we have

$$\nabla \cdot (\rho_0 \nabla \Pi') = -\epsilon t \nabla \cdot (\psi \nabla \Pi), \tag{97}$$

which yields the further estimate

$$\|\Pi'\|_{C^{2,\alpha}} \leqslant \epsilon^2 C\|\psi\|_{C^{1,\alpha}} \tag{98}$$

again independent of t. Then

$$\begin{aligned} d^2(\rho_0, \rho_0 + \epsilon\psi) &\leqslant \int_0^1 \int_\Omega \rho |\nabla \Pi|^2 \,\mathrm{d}x\,\mathrm{d}t \\ &= \epsilon^2 \int_\Omega \rho_0 |\nabla \Phi|^2 \,\mathrm{d}x + \epsilon \int_0^1 \int_\Omega t\psi |\nabla \Pi|^2 \,\mathrm{d}x\,\mathrm{d}t \\ &\quad + \int_0^1 \int_\Omega \rho_0 (2\epsilon \nabla\Phi \cdot \nabla\Pi' + |\nabla \Pi'|^2) \,\mathrm{d}x\,\mathrm{d}t. \end{aligned} \tag{99}$$

It follows from estimates (96) and (98) that

$$d^2(\rho_0, \rho_0 + \epsilon\psi) - \epsilon^2 \int_\Omega \rho_0 |\nabla \Phi|^2 \,\mathrm{d}x \leqslant C\epsilon^3 \tag{100}$$

so that

$$\limsup_{\epsilon \to 0} \frac{d^2(\rho_0, \rho_0 + \epsilon\psi)}{\epsilon^2} \leqslant \int_\Omega \rho_0 |\nabla \Phi|^2 \,\mathrm{d}x. \tag{101}$$

Also note that (96) implies that for any ρ_0, ρ_1, the Wasserstein metric has the bound

$$d^2(\rho_0, \rho_1) \leqslant C\|\rho_0 - \rho_1\|^2_{C^{0,\alpha}}. \tag{102}$$

Lower bound. Let $\bar{v}(x)$ be a velocity field defined by $\bar{v}(x) = \nabla \Pi(x)$ where Π is the solution (again, unique up to a constant) of

$$-\nabla \cdot (\rho_0 \nabla \Pi) = \epsilon\psi, \qquad \frac{\partial \Pi}{\partial n} = 0 \tag{103}$$

which gives the estimate

$$\|v\|_{C^{1,\alpha}} \leqslant \epsilon C\|\psi\|_{C^{1,\alpha}}. \tag{104}$$

Now extend $\bar{v}(x)$ to $v(x,t)$ by letting the velocity be constant along Lagrangian paths as in (82). For small $\bar{v}(y)$, definition (81) and the inverse function theorem imply that there is an inverse map $y(x,t)$ which satisfies

$$y(x,t) = x + y'(x,t), \qquad \|y'\|_{C^{1,\alpha}} \leqslant C\epsilon. \tag{105}$$

Suppose that $\rho(x,t)$ evolves according to $(11_{a,b})$ so that in Lagrangian coordinates, ρ satisfies (86).

We now estimate (86). Using (87) and (105) we can write

$$\nabla_x \cdot v(y(x),t) = \nabla v(y) : \nabla y(x,t) = \nabla \cdot v(y) + \nabla v(y) : \nabla y'(x,t). \tag{106}$$

and using (103) we have

$$\nabla \cdot v(y) = -\frac{\epsilon\psi + v \cdot \nabla \rho_0}{\rho_0}. \tag{107}$$

The exponential term in (86) can be expanded using (106) and (107) as

$$\exp\left(\int_0^t (\nabla_x \cdot v)(y,t)\,\mathrm{d}t\right) = 1 - \frac{\epsilon\psi + v\cdot\nabla\rho_0}{\rho_0} + r(x,t), \tag{108}$$

where, by using (104) and (105), the remainder term r satisfies

$$\|r(x,t)\|_{C^{0,\alpha}} \leqslant C\epsilon^2. \tag{109}$$

Also, using (81) we can expand ρ_0 as

$$\rho_0(y(x,t)) = \rho_0(x) - \nabla\rho_0(x)\cdot v(x) + \rho'(x,t), \tag{110}$$

where by (104) we have

$$\|\rho'\|_{C^{0,\alpha}} \leqslant C\epsilon^2. \tag{111}$$

Now set $\rho^*(x) = \rho(x,1)$, which is, using (86), (108) and (110)

$$\begin{aligned}\rho^*(x) &= \rho_0(y(x,1))\exp\left(\int_0^t (\nabla_x\cdot v)(y,t)\,\mathrm{d}t\right)\\ &= (\rho_0(x) - \nabla\rho_0(x)\cdot v(x) + \rho'(x,t))\left(1 - \frac{\epsilon\psi + v\cdot\nabla\rho_0}{\rho_0} + r(x,t)\right)\\ &= \rho_0(x) + \epsilon\psi(x) + s(x,t),\end{aligned} \tag{112}$$

where by (104), (109) and (111) we have

$$\|s\|_{C^{0,\alpha}} \leqslant C\epsilon^2. \tag{113}$$

Therefore, by defining $\rho_1 = \rho_0 + \epsilon\psi$,

$$\|\rho^* - \rho_1\|_{C^{0,\alpha}} \leqslant C\epsilon^2 \tag{114}$$

and according to the estimate (102),

$$d(\rho^*, \rho_1) \leqslant C\epsilon. \tag{115}$$

Using proposition 2 we have

$$d^2(\rho^0, \rho^*) = \int_\Omega \rho_0(y)|v(y)|^2\,\mathrm{d}y = \epsilon^2\int_\Omega \rho_0(y)|\nabla\Phi|^2\,\mathrm{d}y. \tag{116}$$

It follows from triangle inequality for the Wasserstein metric [44] and (115), (116) that

$$\begin{aligned}d(\rho_0,\rho_1) &\geqslant d(\rho_0,\rho^*) - d(\rho^*,\rho_1)\\ &\geqslant \epsilon\left(\int_\Omega \rho_0|\nabla\Phi|^2\,\mathrm{d}x\right)^{1/2} - C\epsilon^2.\end{aligned} \tag{117}$$

Therefore,

$$\liminf_{\epsilon\to 0}\frac{d^2(\rho_0,\rho_0+\epsilon\psi)}{\epsilon^2} \geqslant \int_\Omega \rho_0|\nabla\Phi|^2\,\mathrm{d}x \tag{118}$$

which establishes the lower bound.

Acknowledgments

The author thanks Paul Fife, who pointed out the inspiring work of Felix Otto, as well as David Eyre and Andrea Bertozzi for useful discussions.

References

[1] Alikakos N D, Bates P W and X Chen 1994 Convergence of the Cahn–Hilliard equation to the Hele–Shaw model *Arch. Rat. Mech. Anal.* **128** 165–205

[2] Almgren R 1996 Singularity formation in Hele–Shaw bubbles *Phys. Fluids* **8** 344

[3] Almgren R, Bertozzi A and Brenner M 1996 Stable and unstable singularities in the unforced Hele–Shaw cell *Phys. Fluids* **8** 1356

[4] Anderson D M and McFadden G B 1997 A diffuse-interface description of internal waves in a near-critical fluid *Phys. Fluids* **9** 1870–79

[5] Anderson D M, McFadden G B and Wheeler A A 1998 Diffuse interface methods in fluid mechanics *Ann. Rev. Fluid. Mech.* **30** 139–65

[6] Antanovskii L K 1995 A phase field model of capillarity *Phys. Fluids* **7** 747–53

[7] Barrett J W, Blowey J F and Garcke H 1999 Finite element approximation of the Cahn–Hilliard equation with degenerate mobility *SIAM J. Numer. Anal.* **37** 286–318

[8] Benamou J-D and Brenier Y 2000 A computational fluid mechanics solution to the Monge–Kantorovich mass transfer problem *Numer. Math.* **84** 375–93

[9] Bernis F and Friedman A 1990 Higher order nonlinear degenerate parabolic equations *J. Diff. Eqns* **83** 179–206

[10] Bertozzi A, Ju N and Glasner K 2002 Nonlinear stability of convexity splitting for fourth order nonlinear diffusion, in preparation

[11] Brenier Y 1991 Polar factorization and monotone rearrangement of vector-valued functions *Commun. Pure Appl. Math.* **64** 375–417

[12] Caginalp G 1986 An analysis of a phase field model of a free boundary *Arch. Rat. Mech. Anal.* **92** 205–45

[13] Caginalp G and Fife P 1988 Dynamics of layered interfaces arising from phase boundaries *SIAM J. Appl. Math.* **48** 506–18

[14] Cahn J W, Elliott C M and Novick-Cohen A 1996 The Cahn-Hilliard equation with a concentration dependent mobility: motion by minus the Laplacian of the mean curvature *Eur. J. Appl. Math.* **7** 287–301

[15] Cahn J W and Hilliard J E 1957 Free energy of a nonuniform system I. Interfacial free energy *J. Chem. Phys.* **28** 258–67

[16] Chella R and Vinals J 1996 Mixing of a two-phase fluid by cavity flow *Phys. Rev.* E **53** 3832–40

[17] Constantin P, Dupont T, Goldstein R, Kadanoff L, Shelley M and Zhou S 1993 Droplet breakup in a model of the Hele–Shaw cell *Phys. Rev.* E **47** 4169

[18] Constantin P and Pugh M 1993 Global solutions for small data to the Hele–Shaw problem *Nonlinearity* **6** 393–415

[19] Diez J A, Kondic L and Bertozzi A 2000 Global models for moving contact lines *Phys. Rev.* E **63** 179–206

[20] Douglas J Jr and Dupont T 1971 Alternating-direction Galerkin methods on rectangles *Numerical Solution of Partial Differential Equations, II (SYNSPADE 1970) (Proc. Symp., University of Maryland, College Park, Md. 1970)* (New York: Academic) pp 133–214

[21] Duchon J and Robert R 1984 Evolution d'une interface par capillaritie et diffusion de volume I. Existence locale en temps *Ann. Inst. H Poincaré* **1** 361–78

[22] Dupont T, Goldstein R E, Kadanoff L P and Zhou S M 1993 Finite-time singularity formation in Hele–Shaw systems *Phys. Rev.* E **47** 4182

[23] Elliott C M and Garcke H 1996 On the Cahn–Hilliard equation with degerate mobility *SIAM J. Math. Anal.* **27** 404–23

[24] Escher J and Simonett G 1997 Classical solutions for Hele–Shaw models with surface tension *Adv. Diff. Eqns* **2** 619–42

[25] Fife P 1991 Seminar, University of Utah

[26] Folch R, Casademunt J, Hernandez-Machado A and Ramirez-Piscina L 1999 Phase-field model for Hele–Shaw flows with arbitrary viscosity contrast I. Theoretical approach *Phys. Rev.* E **60** 1724–32

[27] Gangbo W and McCann R 1996 The geometry of optimal transport *Acta Math.* **177** 113–61

[28] Glasner K 2001 Nonlinear preconditioning for diffuse interfaces *J. Comp. Phys.* **174** 695–711

[29] Goldstein R E, Pesci A and Shelley M J 1998 Instabilities and singularities in Hele–Shaw flow *Phys. Fluids* **10** 2701–23

[30] Grün G 2000 On the convergence of entropy consistent numerical schemes for lubrication-type equations in multiple space dimensions *Preprint*

[31] Gurtin M E, Polignone D and Vinals J 1996 Two phase fluids and immiscible fluids described by and order parameter *Math. Models Methods Appl. Sci.* **6** 815

[32] Hou T Y, Lowengrub J S and Shelley M J 1994 Removing the stiffness from interfacial flows with surface tension *J. Comp. Phys.* **114** 312

[33] Jackson D P and Goldstein R E 1994 Hydrodynamics of fingering instabilities in dipolar fluids *Phys. Rev.* E **50** 298–307
[34] Jacqmin D 1999 Computation of two-phase Navier–Stokes flows using phase field modeling *J. Comp. Phys.* **155** 96–127
[35] Jacqmin D 1999 Contact line dynamics of a diffuse fluid interface *J. Fluid. Mech.* **402** 57–88
[36] Kantorovich L 1948 On a problem of Monge *Usp Mat. Nauk.* **3** 225–6
[37] Kohn R V and Otto F 1997 Small surface energy, coarse-graining, and selection of microstructure *Physica* D **107** 272–89
[38] Korteweg D 1901 Sur la forme que prennent les equations du mouvements des fluides si l'on tient compte des forces capillaires causees par les variations de densite consierables et sur la theorie da la capillarite dans l'hypothese d'une variation continue de la densite *Arch. Neerl. Sci. Exactes Nat. Ser. II* **6** 1–24
[39] Lee H G, Lowengrub J S and Goodman J 2002 Modelling pinchoff and reconnection in a Hele–Shaw cell I: the models and their calibration *Phys. Fluids* **14** 492–513
[40] Lee H G, Lowengrub J S and Goodman J 2002 Modelling pinchoff and reconnection in a Hele–Shaw cell II: analysis and simulation in the non-linear regime *Phys. Fluids* **14** 514–45
[41] Lowengrub J and Truskinovsky L 1998 Quasi-incompressible Cahn–Hilliard fluids and topological transitions *Proc. R. Soc.* A **454** 2617–54
[42] Monge G 1781 Memoire sur la theorie des deblais et de remblais *Histoire de l'Acadamie Royale des Sciences de Paris, avec les Memories de Mathematique et de Physique pour la meme annee* pp 666–704
[43] Oron A, Davis S H and Bankoff S G 1997 Long-scale evolution of thin liquid films *Rev. Mod. Phys.* **69** 931–80
[44] Otto F 1998 Dynamics of labrinthine pattern formation in magnetic fluids: a mean-field theory *Arch. Rat. Mech. Anal.* **141** 63–103
[45] Otto F 1998 Lubrication approximation with prescribed nonzero contact angle *Commun. Partial Diff. Eqns* **23** 2077–164
[46] Otto F 2001 The geometry of dissipative evolution equations: the porous medium equation *Commun. Partial Diff. Eqns* **26** 101–74
[47] Pego R L 1989 Front migration in the nonlinear Cahn–Hilliard equation *Proc. R. Soc. Lond.* A **422** 261–78
[48] Prokert G 1998 Existence results for Hele–Shaw flow driven by surface tension *Eur. J. Appl. Math.* 8 195–221
[49] Smereka P 2002 Semi-implicit level set methods for curvature and surface diffusion motion *Preprint*
[50] Taylor J, Cahn J and Handwerker C 1992 Geometric models of crystal growth *Acta. Metal. Mater.* **40** 1–39
[51] Tryggvason G and Aref H 1983 Numerical experiments on Hele–Shaw flow with a sharp interface *J. Fluid Mech.* **136** 1–30
[52] van der Waals J D 1893 The thermodynamic theory of capillary flow under the hypothesis of a continuous variation of density (Amsterdam: Verhadel Konink Akad. Weten.) p 1
[53] Wheeler A A, Boettinger W and McFadden G 1992 Phase-field model for isothermal transitions in binary alloys *Phys. Rev.* A **45** 7424–39
[54] Wheeler A A, Boettinger W and McFadden G 1992 Phase-field model for solidification of a eutectic alloy *Proc. R. Soc.* A **452** 495